Ultrasound in Med. & Biol., Vol. 33, No. 2, pp. 311–317, 2007

0301-5629/07/$–see front matter

ELSEVIER

doi:10.1016/j.ultrasmedbio.2006.08.015

● *Original Contribution*

HEMORRHAGE NEAR FETAL RAT BONE EXPOSED TO PULSED ULTRASOUND

TIMOTHY A. BIGELOW,*† RITA J. MILLER,† JAMES P. BLUE, JR.,† and WILLIAM D. O'BRIEN, JR.†

*Department of Electrical Engineering, University of North Dakota, Grand Forks, ND, USA; and †Bioacoustics Research Laboratory, Department of Electrical and Computer Engineering, University of Illinois at Urbana-Champaign, Urbana, IL, USA

(*Received* 9 *February* 2006; *revised* 3 *August* 2006; *in final form* 10 *August* 2006)

Abstract—Ultrasound-induced hemorrhage near the fetal rat skull was investigated to determine if the damage could be correlated with temporal-average intensity. A 0.92-MHz f/1 spherically focused transducer (5.1-cm focal length) was used to expose the skull of 18- to 19-day gestation exteriorized Sprague-Dawley rat fetuses (n = 197). There were four ultrasound-exposed groups (n = 36 each), one sham exposed group (n = 36) and one cage control group (n = 17). Three of the ultrasound-exposed groups had the same peak compressional (10 MPa)/peak rarefactional (6.7 MPa) pressure but different spatial-peak temporal-average intensities (I_{TA}) of 1.9, 4.7 and 9.4 W/cm^2; the pulse repetition frequency (PRF) was varied (100, 250 and 500 Hz, respectively). The fourth ultrasound-exposed group had a peak compressional (6.7 MPa)/peak rarefactional (5.0 MPa) pressure and corresponding I_{TA} of 4.6 W/cm^2; PRF was 500 Hz. Hemorrhage occurrence increased slightly with increasing I_{TA}, as well as peak rarefactional pressure and PRF, but the hemorrhage area did not correlate with any of the exposure parameters. (E-mail: timothybigelow@mail.und.nodak.edu) **© 2007 World Federation for Ultrasound in Medicine & Biology.**

Key Words: **Ultrasound bioeffects, Rat, Fetal bone, Hemorrhage.**

INTRODUCTION

In addition to its long history in diagnostic applications, ultrasound at high intensities also has been used in therapeutic applications. A principal advantage of using ultrasound in treating ailments has been its ability to noninvasively target specific regions of interest at depth without affecting the interposed tissue. This selective targeting capability is a great advantage when other treatment options, such as surgery, are not possible or greatly increase the risk to the patient. Ultrasound therapy often involves thermal ablation where tissue necrosis is induced by elevated temperatures (Foley et al. 2004; Hynynen 1997; Lizzi et al. 1992; Otsuka et al. 2005; Souchon et al. 2003; Takegami et al. 2005; Wu et al. 2004). Ultrasound also has been used to remove tissue in a controlled manner (Xu et al. 2004, 2005), gene transfection (Christiansen et al. 2003; Zarnitsyn and Prausnitz 2004), localized drug delivery (Shortencarier et al. 2004) and the acceleration of thrombolysis (Everbach and Francis 2000).

One ultrasound therapy application that has received relatively little attention is use on or near the developing fetus. However, before the use of ultrasound therapy can be safely explored on or near the fetus, the potential risk of ultrasound-induced bioeffects on the fetus needs to be better understood so that unintended bioeffects can be avoided or minimized when using ultrasound for thermal ablation or gene/drug delivery, for example. Although there have been considerable studies of ultrasound-induced fetal-related thermal bioeffects (Barnett 2000; Duggan et al. 1995; Edwards et al. 1995; Herman and Harris 2002, 2003; Horder et al. 1998; Mazza et al. 2004; Miller and Dewey 2003; Miller et al. 2002, 2004; Miller and Ziskin 1989; Stone et al. 1992), not all bioeffects may result from heating. One harmful bioeffect that has received relatively little attention is ultrasound-induced hemorrhage near the fetal skull, an effect that should be avoided when using ultrasound for therapy applications.

Ultrasound-induced hemorrhage near the mouse fetal skull has been observed from lithotripter (Dalecki et

Address correspondence to: Timothy A. Bigelow, Department of Electrical Engineering, University of North Dakota, Box 7165, Grand Forks, ND 58202, USA. E-mail: timothybigelow@mail.und.nodak.edu

al. 1997) and single-element ultrasound pulsed exposures (Dalecki et al. 1999). The authors of these studies claimed that the hemorrhage did not result from heating because the occurrence of hemorrhage did not increase with increasing frequency (Dalecki et al. 1999). They did not explain, however, why they would expect the heating of bone to increase with the higher frequency sources used in their experiment. Although absorption of bone does increase with frequency, they neglected the role of beam width on the heating of bone. In their investigation, the higher frequency transducers had smaller beam widths. As the beam width is reduced, the temperature rise resulting from ultrasound absorption also should decrease (Carstensen et al. 1990; Vella et al. 2003). Instead of heating, the authors attributed the hemorrhage to relative motion between partially ossified bone and the surrounding tissue resulting from radiation force. However, their argument is not completely convincing because the force resulting from ultrasound would be much smaller than the force on the skull during normal delivery.

The frequency dependence of the observed hemorrhage suggests that cavitation might be the mechanism responsible for the bioeffect because the likelihood of inertial cavitation decreases with increasing frequency (Apfel and Holland 1991). Although some have argued that any occurrence of hemorrhage is due to cavitation (Carstensen et al. 1992), ultrasound-induced lung hemorrhage, for example, has been shown not to result from inertial cavitation (O'Brien et al. 2000). Dalecki et al. (1999) dismissed cavitation as a possible mechanism because cavitation nuclei are typically not present in tissue (Carstensen et al. 2000). However, despite the lack of known nuclei in tissue, cavitation has been observed in human tissue (Coleman et al. 1995). Furthermore, the collapse of a microbubble near bone might result in increased tissue damage due to the formation of a microjet (Brujan 2004; Gracewski et al. 2005). Microjets form due to the asymmetric collapse of the bubbles near boundaries and can be used to erode metals (Blake and Gibson 1987; Chiu et al. 2005; Pearson et al. 2004). Microjets could potentially damage the vasculature if a blood vessel is sufficiently close to the bone, which would be the case for developing bone. The inner layer of the periosteum, which contains the osteoblasts for developing bone, is highly vascularized and is the major component for blood flow in the developing bone. The vascularization of the periosteum decreases as the bone matures. Therefore, cavitation also needs to be investigated as a possible mechanism for hemorrhage near developing fetal bone.

The goal of this study was to provide more experimental evidence of hemorrhage near fetal bone resulting from ultrasound exposure to determine if the hemorrhage could at least be correlated with the spatial-peak temporal-average intensity (temperature or radiation force type mechanism) or peak rarefactional pressure (cavitation type mechanism). If the damage correlates with the spatial-peak temporal-average intensity, the risk of hemorrhage might be estimated in the same way the risk of heating is assessed. Our goal was not to conclusively determine the mechanism responsible for the observed damage, as this would not be possible using the results from a single study.

Table 1. Overview of exposure conditions.

Exposure	p_c, p_r (MPa)	PRF	I_{TA}
Alignment, Sham	1.1, 1.1	25 Hz	6.9 mW/cm^2
A	10.2, 6.7	100 Hz	1.9 W/cm^2
B	10.2, 6.7	250 Hz	4.7 W/cm^2
C	10.2, 6.7	500 Hz	9.4 W/cm^2
D	6.7, 5.0	500 Hz	4.6 W/cm^2

Experiment Protocol

The experimental protocol was approved by the Institutional Animal Care and Use Committee at the University of Illinois at Urbana-Champaign and satisfied all campus and NIH rules for the humane use of laboratory animals.

Pregnant Sprague-Dawley rats (Harlan, Indianapolis, IN) with a gestational age of 18 to 19 d were anesthetized with ketamine hydrochloride (87.0 mg/kg) and xylazine (13.0 mg/kg) administered intramuscularly. The pregnant rats were placed in dorsal recumbency, and their abdomens shaved. Incisions were made in the pelvic region; the tissue layers were pulled back revealing the uterus containing the developing fetuses. A standoff vessel containing 37°C degassed water was gently positioned in contact with the uterus, and mineral oil was used as a coupling agent on the uterine surface. The ultrasound beam axis for an f/1 (5.1-cm focal length) 0.92-MHz spherically focused transducer (Matec/Valpey Fisher Instruments, Inc., Hopkinton, MA) was then visually aligned through the uterus over the fetal skull. The focus was positioned at the fetal skull by maximizing the reflection at the focal depth from a low-amplitude pulse with a pulse duration (PD) of 12.3 μs (*i.e.*, alignment exposure).

After alignment, the fetuses were randomly exposed to one of four different ultrasound exposures (denoted A, B, C and D) using a PD of 9.6 μs or a sham exposure for an exposure duration of 60 s. The exposure conditions, including the alignment exposure as measured with a calibrated membrane hydrophone (Marconi, Ltd., Essex, England) in a water bath, are provided in Table 1. For three of the four exposures (A, B and C), the peak

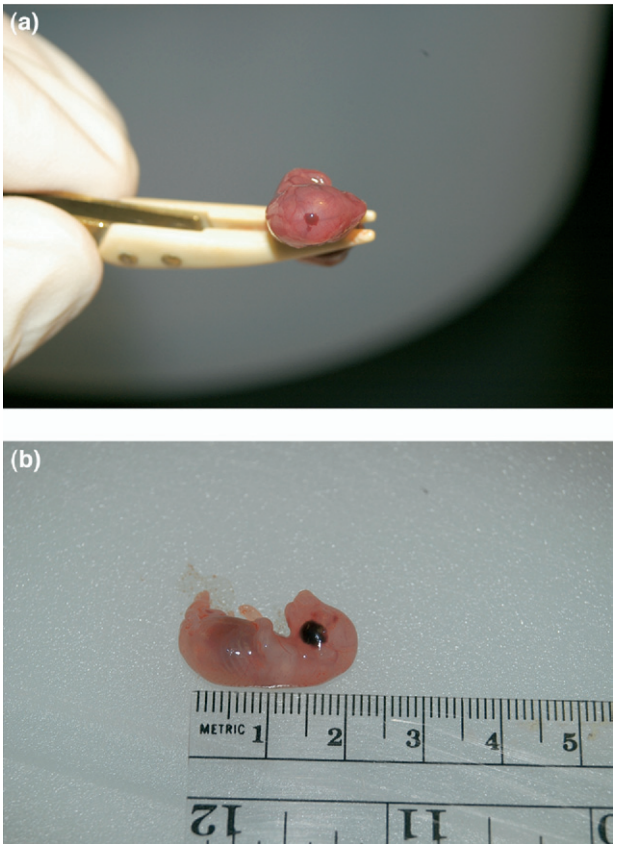

Fig. 1. Images showing two different hemorrhages on fetal heads resulting from ultrasound exposure.

compressional pressure (p_c) and the peak rarefactional pressure (p_r) were the same (*i.e.*, 10.2 and 6.7 MPa, respectively). The spatial-peak temporal-average intensities (I_{TA}) were varied by changing the pulse repetition frequency (PRF). If hemorrhage correlated with ultrasound pressure, all three of these exposures should result in approximately the same hemorrhage occurrence and size. In addition, exposures B and D had approximately the same I_{TA}, but different p_c and p_r values. Hence, the hemorrhage occurrence and size for exposures B and D should be very similar if hemorrhage correlated with I_{TA}.

Thirty-six fetuses (corresponding to 15 mothers) were used for each ultrasound or sham exposure for a total of 180 fetuses. The exposure conditions for the fetuses were randomized (~ two fetuses per exposure condition per mother). Following fetal exposures, the mother and fetuses were humanely euthanized while under anesthesia, and the fetuses were examined for tissue hemorrhage. Examples of the hemorrhage observed on the fetuses are shown in Fig. 1. In addition to the 180 fetuses, two pregnant rats were anesthetized and humanely euthanized without exteriorizing the fetuses or exposing them to ultrasound (17 total in secondary control group; cage controls). These 17 fetuses were also assessed for hemorrhages. The individuals responsible for alignment of the transducer and assessing the hemorrhaging remained blinded to the exposure conditions until completion of the study.

RESULTS

The percentage of hemorrhage occurrences for the fetuses at exposures I_{TA}, p_r and PRF are shown in Fig. 2 and summarized in Table 2. The results are plotted by comparing $I_{TA}$and p_r with PRF because cavitation damage has been shown to be more significant at higher PRFs (Chang et al. 2001; Chen et al. 2003; Madanshetty et al. 1991). If cavitation is the mechanism responsible for the hemorrhage, then the hemorrhage should be enhanced at higher PRFs and higher p_r's. The solid line denotes hemorrhage occurrences anywhere on the body of the fetus, and the dashed line denotes hemorrhage occurrences on the fetal head only. Hemorrhage was expected on the fetal head because the ultrasound beam should have been aligned with the fetal skull. The hemorrhage occurrence in the sham exposures (Table 1) and the absence of hemorrhage in secondary control group (all zero) might indicate that the alignment exposure generated some hemorrhage. However, the occurrence in the sham exposures also could have resulted from an adjacent fetus moving into the path of the ultrasound beam, which will be considered in the Discussion. Another possibility is that exteriorizing the fetuses increased the stress experienced by the fetus and that resulted in some hemorrhage. Fetal motion and fetal stress are more likely culprits than the sham exposure for producing hemorrhage because exposure A (all-body hemorrhage occurrence of 11%) had approximately the same occurrence as that of the sham exposures (all-body hemorrhage occurrence of 14%).

There is a monotonic increase in hemorrhage occurrence as I_{TA} increases (Fig. 2a), but no such increase in the sham exposures, indicating a possible dependence on temporal-average intensity. Hemorrhage occurrence for the 4.6 W/cm^2- exposure (D) is different than the 4.7 W/cm^2-exposure (B), but the difference is on the same order as hemorrhage occurrence in the sham exposures, suggesting a possible correlation with I_{TA}.

Hemorrhage occurrence does not correlate with p_r (Fig. 2b) due to the large variation in occurrence at a p_r of 6.7 MPa (A, B and C). However, exposure C (p_r of 6.7 MPa) results in a larger occurrence than exposure D (p_r of 5.0 MPa) when the same PRF of 500 Hz is used. Also, hemorrhage occurrence increases monotonically with increasing PRF (Fig. 2c), with the exception of exposure D, which corresponds to a smaller p_r. Therefore, hemorrhage occurrence increases when p_r and PRF are consid-

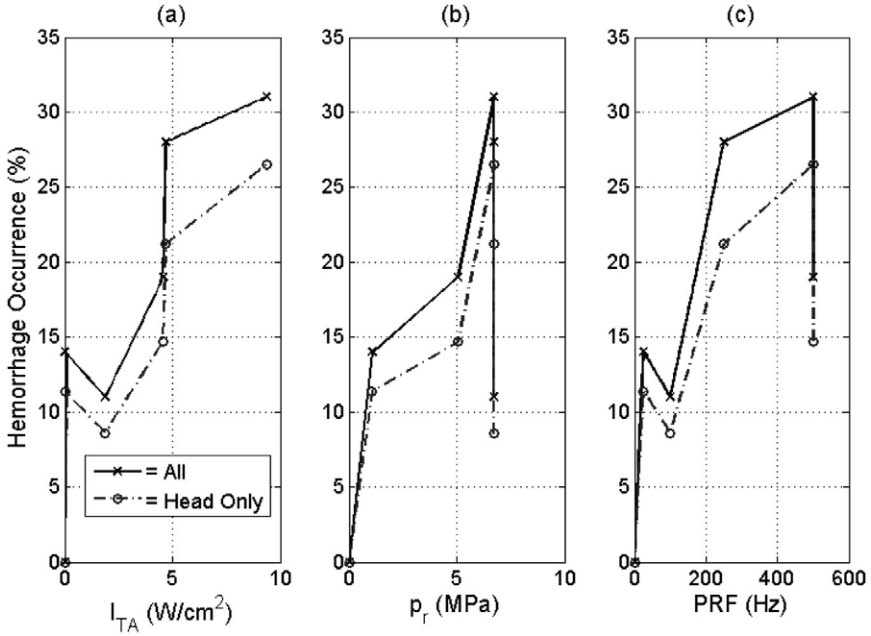

Fig. 2. Hemorrhage occurrence *vs.* (a) spatial-peak temporal-average intensity, I_{TA}; (b) peak rarefactional pressure, p_r; (c) pulse repetition frequency, PRF. The solid line denotes hemorrhage occurrences anywhere on the body of the fetus. The dashed line denotes hemorrhage occurrences on the fetal head only.

ered together, suggesting cavitation as a possible mechanism.

In addition to hemorrhage occurrence, the damage also is quantified by estimating the hemorrhaged surface area by an ellipse and measuring the major and minor axes. Figure 3 illustrates the largest (upper error bar), smallest (lower error bar), and mean hemorrhage area as functions of I_{TA}, p_r and PRF. Although there are large variations in the hemorrhage area, the largest hemorrhages occur for exposure D, which has a pressure and temporal-average intensity in the middle of the ranges considered, whereas the other exposures yield approximately the same hemorrhage sizes. Hence, the hemorrhage area does not correlate with I_{TA}, p_r or PRF.

DISCUSSION

Hemorrhage occurrence generally increased with I_{TA} as well as p_r and PRF when compared together, whereas hemorrhage area did not increase. Hence, the mechanism responsible for hemorrhage initiation might be different from the mechanism responsible for hemorrhage growth. The overall low hemorrhage occurrence also was surprising given the exposure conditions used in this study. The lack of correlation between hemorrhage area and I_{TA} or p_r and PRF, as well as the reduced hemorrhage occurrence, might be related to fetal motion. After positioning the uterus containing the fetus and aligning the transducer, the fetus could move. The fetal movement also could cause the fetus to move out of the path of the ultrasound beam. In the worst-case scenario, an adjacent fetus might shift into the beam because of the proximity of the fetuses in the uterus. This also could explain hemorrhage occurrence in some of the sham exposures, as well as the hemorrhage at locations other than the fetal head. Minimally, the same location on the fetus would not be exposed for the entire time if fetal movement occurred.

Table 2. Hemorrhage occurrence and area (mean ± standard deviation) summary.

Exposure	All-body occurrence (%)	Skull occurrence (%)	All-body area (mm^2)	Skull area (mm^2)
Alignment, Sham	14	11	2.6 ± 2.8	1.8 ± 2.6
A	11	9	3.1 ± 3.4	1.4 ± 0.76
B	28	21	2.5 ± 2.6	2.3 ± 2.9
C	31	27	2.7 ± 3.4	2.0 ± 3.1
D	19	15	5.1 ± 4.4	4.1 ± 4.9

Some fetal movement could be detected by monitoring the backscattered waveform during the ultrasound exposure if the reflected waveform did not saturate the receiver. The receiver gain was set to monitor the alignment echoes and not the exposure echoes. In this study, fetal movement was observed in 14/26 (54%) of the echoes that did not saturate the receiver for exposure A, 11/23 (48%) for exposure B, 14/19 (74%) for exposure C and 11/28 (39%) for exposure D. The mean hemorrhage area tended to decrease as the perceived fetal movement

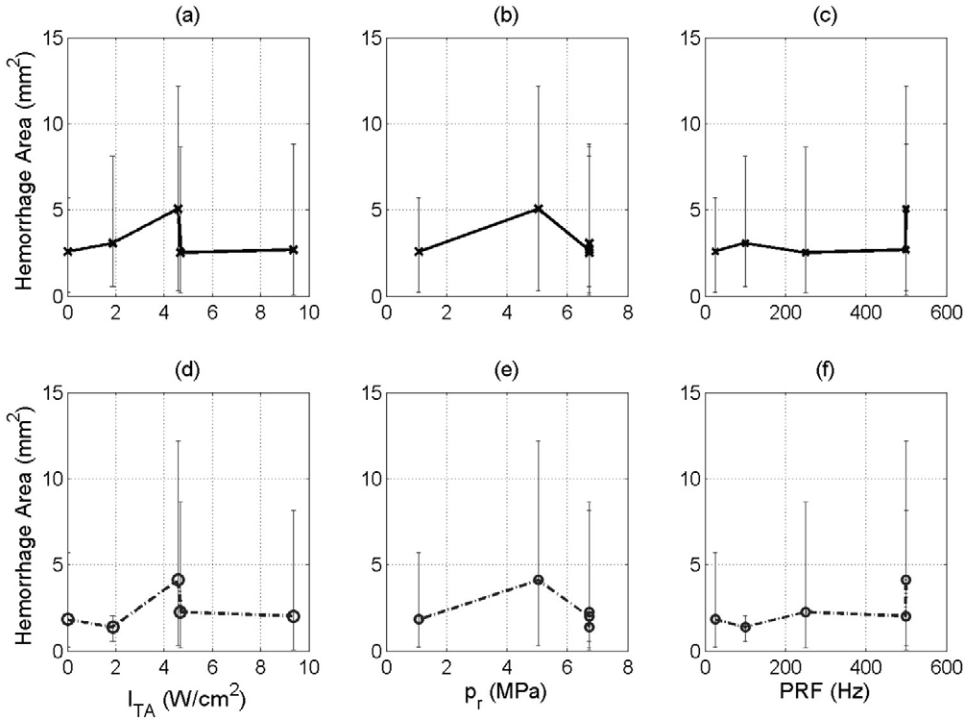

Fig. 3. Hemorrhage area for (a) all body locations *vs.* I_{TA}; (b) all body locations *vs.* p_r; (c) all body locations *vs.* PRF; (d) head-only locations *vs.* I_{TA}; (e) head-only locations *vs.* p_r; (f) head-only locations *vs.* PRF.

increased (Fig. 4). Hence, the hemorrhage area appeared to correlate with fetal movement.

Hemorrhage occurrence increased as a function of I_{TA} (Fig. 2a), suggesting a thermal or radiation force mechanism. To examine the possibility of a thermal mechanism further, an approximate temperature increase was calculated. The temperature increase as a function of time, t, for heating of the fetal skull, assuming all of the heating is due to sound absorption in an infinitesimally thin layer, is approximately given by (Carstensen et al. 1990)

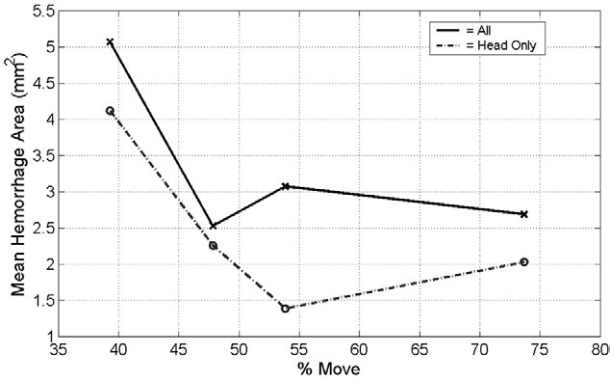

Fig. 4. Hemorrhage area *vs.* perceived fetal movement.

$$T(t) = \int_0^\infty \frac{\phi I(r)}{4K}\left\{e^{-r/L}\left[2 - erfc\left(\sqrt{t/\tau} - r/\sqrt{4\kappa t}\right)\right] + e^{r/L}erfc\left(\sqrt{t/\tau} + r/\sqrt{4\kappa t}\right)\right\}dr, \quad (1)$$

where κ is the thermal diffusivity of the medium; τ is the time constant for perfusion; L is the perfusion length ($L = \sqrt{\kappa\tau}$), K is the thermal conductivity coefficient; ϕ is a dimensionless constant that gives the fraction of the incident intensity that is absorbed; r is the radial distance perpendicular to the beam axis (along the thin bone layer where the sound is absorbed); $I(r)$ is the incident temporal-average intensity at r assuming circular symmetry about the beam axis. For the calculation, $K = 0.6$ W/m−°C; $\kappa = 1.4 \times 10^{-7}$ m^2/s, $\tau = 100$ s, and $\phi = 0.6$ (Carstensen et al. 1990). $I(r)$ used in the calculation was given by

$$I(r) = I_{TA}\left[\frac{2J_1\left(\frac{\pi r}{\lambda(f\#)}\right)}{\frac{\pi r}{\lambda(f\#)}}\right]^2, \quad (2)$$

where the location of I_{TA} is at the focus that was measured for each exposure condition; λ is the wavelength of

the sound (corresponding to 0.92 MHz); *f#* is the f-number for the source (*i.e.*, 1 for our study).

The calculated temperature increases as a function of time associated with the four exposures (A, B, C and D), which are shown in Fig. 5. The maximum temperature increase for the alignment exposure (not shown) was 0.026°C. Significant temperature increases are expected relatively quickly for all four of the exposure conditions assuming the beam is incident on bone. In addition, the hemorrhage occurrences, C>B>D>A, (Table 2) correlate with the calculated temperature increases, C>B≈D>A, where, for example, the exposure with the highest temperature also had the largest hemorrhage occurrence.

To further investigate the possibility of heating as a mechanism, the temperature increases resulting from three of the exposures in the work of Dalecki and colleagues (1999) also were calculated using the same assumptions and their reported ultrasound focal intensities. The 100-Hz PRF, 10-μs PD fetal mouse exposures from their work that we considered were 1.2 MHz (I_{TA} = 1.3 W/cm^2; hemorrhage occurrence of 40%), 2.4 MHz (I_{TA} = 1.5 W/cm^2; hemorrhage occurrence of 13%) and 3.6 MHz (I_{TA} = 1.2 W/cm^2; hemorrhage occurrence of 6%). Dalecki and colleagues (1999) found sham exposures with a hemorrhage occurrence of 3.5% to 7%. Although less heating is expected from the exposures used in their study, the hemorrhage occurrences that they found, 1.2 MHz > 2.4 MHz > 3.6 MHz, directly correlated with the estimated temperature increases (Fig. 6). Hence, the frequency dependence observed in their study might be due to a beam width dependence, and the hemorrhage might be due to heating.

Although heating is a possible mechanism for the observed hemorrhage, the damage might be due to cavitation. Cavitation would agree with the generally observed dependence on p_r and PRF in our study, as well as the frequency dependence in the work of Dalecki and colleagues (1999), because the likelihood of inertial cavitation decreases with increasing frequency (Apfel and Holland 1991). Therefore, more experiments are needed before the mechanism(s) responsible for the occurrence and severity of the hemorrhage can be identified.

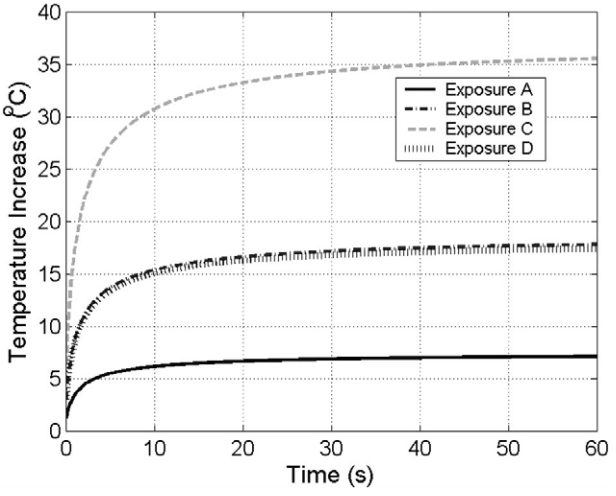

Fig. 5. Estimated temperature increase for ultrasound exposures used in our study.

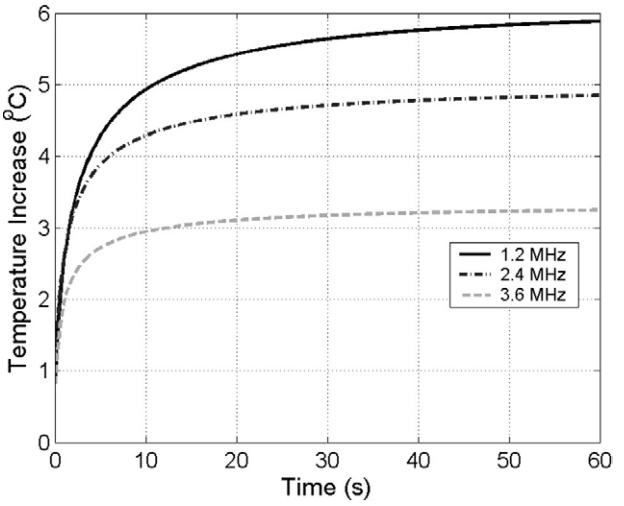

Fig. 6. Estimated temperature increase for three of the ultrasound exposures used by Dalecki et al. (1999).

Acknowledgements—The authors thank Z. Hafez for his technical contributions. This work was supported by the University of Illinois Research Board, NIH R37EB02641, and the University of North Dakota School of Engineering and Mines.

REFERENCES

Apfel RE, Holland CK. Gauging the likelihood of cavitation from short-pulse, low-duty cycle diagnostic ultrasound. Ultrasound Med Biol 1991;17:179–185.

Barnett SB. Biophysical aspects of diagnostic ultrasound. Ultrasound Med Biol 2000;26(S1):S68–S70.

Blake JR, Gibson DC. Cavitation bubbles near boundaries. Annual review of fluid mechanics. Annu Rev Fluid Mech 1987;19:99–123.

Brujan EA. The role of cavitation microjets in the therapeutic applications of ultrasound. Ultrasound Med Biol 2004;30:381–387.

Carstensen EL, Child SZ, Norton S, et al. Ultrasonic heating of the skull. J Acoust Soc Am 1990;87:1310–1317.

Carstensen EL, Duck FA, Meltzer RS, et al. Bioeffects in echocardiography. Echocardiography 1992;9:605–623.

Carstensen EL, Gracewski S, Dalecki D. The search for cavitation in vivo. Ultrasound Med Biol 2000;26:1377–1385.

Chang PP, Wen-Shiang C, Mourad PD, et al. Thresholds for inertial cavitation in Albunex suspensions under pulsed ultrasound conditions. Ultrasonics, IEEE Trans Ultrason Ferroelect Freq Contr 2001;48:161–170.

Chen W-S, Brayman AA, Matula TJ, et al. The pulse length-dependence of inertial cavitation dose and hemolysis. Ultrasound Med Biol 2003;29:739–748.

Chiu KY, Cheng FT, Man HC. Evolution of surface roughness of some metallic materials in cavitation erosion. Ultrasonics 2005;43:713–716.

Christiansen JP, French BA, Klibanov AL, et al. Targeted tissue transfection with ultrasound destruction of plasmid-bearing cationic microbubbles. Ultrasound Med Biol 2003;29:1759–1767.

Coleman AJ, Kodama T, Choi MJ, et al. The cavitation threshold of human tissue exposed to 0.2-MHz pulsed ultrasound: Preliminary measurements based on a study of clinical lithotripsy. Ultrasound Med Biol 1995;21:405–417.

Dalecki D, Child SZ, Raeman CH, et al. Thresholds for fetal hemorrhages produced by a piezoelectric lithotripter. Ultrasound Med Biol 1997;23:287–297.

Dalecki D, Child SZ, Raeman CH, et al. Hemorrhage in murine fetuses exposed to pulsed ultrasound. Ultrasound Med Biol 1999;25:1139–1144.

Duggan PM, Liggins GC, Barnett SB. Ultrasonic heating of the brain of the fetal sheep in utero. Ultrasound Med Biol 1995;21:553–560.

Edwards MJ, Shiota K, Smith MSR, et al. Hyperthermia and birth defects. Repro Toxicol 1995;9:411–425.

Everbach EC, Francis CW. Cavitational mechanisms in ultrasound-accelerated thrombolysis at 1 MHz. Ultrasound Med Biol 2000;26:1153–1160.

Foley JL, Little JW, Starr IIIFL, et al. Image-guided HIFU neurolysis of peripheral nerves to treat spasticity and pain. Ultrasound Med Biol 2004;30:1199–1207.

Gracewski SM, Miao H, Dalecki D. Ultrasonic excitation of a bubble near a rigid or deformable sphere: Implications for ultrasonically induced hemolysis. J Acoust Soc Am 2005;117:1440–1447.

Herman BA, Harris GR. Models and regulatory considerations for transient temperature rise during diagnostic ultrasound pulses. Ultrasound Med Biol 2002;28:1217–1224.

Herman BA, Harris GR. Response to "An extended commentary on 'Models and regulatory considerations for transient temperature rise during diagnostic ultrasound pulses' by Herman and Harris (2002). Ultrasound Med Biol 2003;29:1661–1662.

Horder MM, Barnett SB, Vella GJ, et al. Effects of pulsed ultrasound on sphenoid bone temperature and the heart rate in guinea-pig foetuses. Early Hum Dev 1998;52:221–233.

Hynynen K. Review of ultrasound therapy. IEEE Ultrasonics Symposium 1997;2:1305–1313.

Lizzi FL, Driller J, Lunzer B, et al. Computer model of ultrasonic hyperthermia and ablation for ocular tumors using b-mode data. Ultrasound Med Biol 1992;18:59–73.

Madanshetty SI, Roy RA, Apfel RE. Acoustic microcavitation: Its active and passive acoustic detection. J Acoust Soc Am 1991;90:1515–1526.

Mazza S, Battaglia LF, Miller MW, et al. The [δ]T thermal dose concept 2: in vitro cellular effects. J Thermal Biology 2004;29:151–156.

Miller MW, Dewey WC. An extended commentary on "Models and regulatory considerations for transient temperature rise during diagnostic ultrasound pulses" by Herman and Harris (2002). Ultrasound Med Biol 2003;29:1653–1659.

Miller MW, Nyborg WL, Dewey WC, et al. Hyperthermia teratogenicity, thermal dose and diagnostic ultrasound during pregnancy: implications of new standards on tissue heating. Int J Hyperthermia 2002;18:361–384.

Miller MW, Miller RK, Battaglia LF, et al. The [δ]T thermal dose concept 1: In vivo teratogenesis. J Thermal Biology 2004;29:141–149.

Miller MW, Ziskin MC. Biological consequences of hyperthermia. Ultrasound Med Biol 1989;15:707–722.

O'Brien WD Jr, Frizzell LA, Weigel RM, et al. Ultrasound-induced lung hemorrhage is not caused by inertial cavitation. J Acoust Soc Am 2000;108:1290–1297.

Otsuka R, Fujikura K, Hirata K, et al. In vitro ablation of cardiac valves using high-intensity focused ultrasound. Ultrasound Med Biol 2005;31:109–114.

Pearson A, Blake JR, Otto SR. Jets in bubbles. J Engineering Mathematics 2004;48:391–412.

Shortencarier MJ, Dayton PA, Bloch SH, et al. A method for radiation-force localized drug delivery using gas-filled lipospheres. Ultrasonics, IEEE Trans Ultrason Ferroelect Freq Contr 2004;51:822–831.

Souchon R, Rouviere O, Gelet A, et al. Visualisation of HIFU lesions using elastography of the human prostate in vivo: preliminary results. Ultrasound Med Biol 2003;29:1007–1015.

Stone PR, Ross I, Pringle K, et al. Tissue heating effect of pulsed Doppler ultrasound in the live fetal lamb brain. Fetal Diagn Ther 1992;7:26–30.

Takegami K, Kaneko Y, Watanabe T, et al. Erythrocytes, as well as microbubble contrast agents, are important factors in improving thermal and therapeutic effects of high-intensity focused ultrasound. Ultrasound Med Biol 2005;31:385–390.

Vella GJ, Humphrey VF, Duck FA, et al. Ultrasound-induced heating in a foetal skull bone phantom and its dependence on beam width and perfusion. Ultrasound Med Biol 2003;29:779–788.

Wu F, Wang Z-B, Lu P, et al. Activated anti-tumor immunity in cancer patients after high intensity focused ultrasound ablation. Ultrasound Med Biol 2004;30:1217–1222.

Xu Z, Ludomirsky A, Eun LY, et al. Controlled ultrasound tissue erosion. Ultrasonics, IEEE Trans Ultrason Ferroelect Freq Contr 2004;51:726–736.

Xu Z, Fowlkes JB, Rothman ED, et al. Controlled ultrasound tissue erosion: The role of dynamic interaction between insonation and microbubble activity. J Acoust Soc Am 2005;117:424–435.

Zarnitsyn VG, Prausnitz MR. Physical parameters influencing optimization of ultrasound-mediated DNA transfection. Ultrasound Med Biol 2004;30:527–538.